

Multimode and multifrequency gigahertz surface acoustic wave sensors

Werner Seidel and Thorsten Hesjedal^{a)}

Paul-Drude-Institut für Festkörperelektronik, Hausvogteiplatz 5-7, D-10117 Berlin, Germany

(Received 13 October 2003; accepted 23 December 2003)

A simple surface acoustic wave sensor system is presented that combines the advantages of multifrequency/multimode operation and GHz frequencies in a single acoustic device structure. Analyzing multiple frequencies and modes is the basis for the multicomponent analysis of gases and liquids. The sensor system is based on floating electrode unidirectional transducers that allow efficient excitation of two modes and up to 48 harmonics (or 5 GHz). It can be fabricated without the need of costly nanofabrication techniques. Higher sensor frequencies are advantageous as the sensitivity increases with the frequency. We tested the basic operation of our sensor system by applying it to humidity sensing without a sensitive layer. © 2004 American Institute of Physics. [DOI: 10.1063/1.1650040]

As surface acoustic waves (SAWs) are localized in the vicinity of the surface, their propagation properties are altered in response to any change in mechanical or electrical boundary conditions. The resulting changes in velocity and attenuation of the SAW are measures of the amount and physical properties of absorbed chemical species. This makes SAWs suitable probes for sensing applications^{1,2} ranging from simple humidity sensors to more complex gas sensors and even liquid biosensors.³ Due to their wireless read-out capability, SAW sensors are also attractive for automotive applications such as angular rate sensors, pressure sensors, and liquid sensors in harsh environments.⁴ For practical application the SAW resonators are usually coated with thin analyte-selective layers in order to enhance their specificity. In general, the sensor sensitivity $\Delta f/f$ to a mass load is proportional to the frequency f , which has been verified experimentally.⁵ Consequently, the limits of detectability may be lowered by higher operation frequencies.

High frequencies, i.e., short wavelengths and thus a stronger SAW localization at the surface, also offer the possibility to efficiently probe the viscoelastic properties of the sensing layers. In addition, thinner coatings down to monolayers can be employed, leading to shorter response times. In a multifrequency/multimode setup especially, the parallel readout of several frequencies and modes and their different responses offer the possibility of selective chemical detection and materials characterization.⁶ Therefore, higher operation frequencies are a promising strategy for better sensors, and are only limited by the photolithographic process. Unfortunately, the frequency range beyond 1 GHz is difficult to reach employing simple photolithography for SAW transducer fabrication.

Here, we report on a SAW sensor system that combines the advantages of high-frequency operation in the GHz range with multifrequency and multimode excitation in a single device. By employing a special unidirectional SAW device, so-called floating electrode unidirectional transducers (FEUDTs), a set of harmonic frequencies, ranging from $f_0 = 0.105$ GHz to $f_{48} = 5.005$ GHz for the first mode and from

$f_0 = 0.121$ GHz to $f_{13} = 1.452$ GHz for the second mode, can be efficiently excited. FEUDTs can be fabricated without the need of costly nanolithography.⁷ The basic performance of the uncoated FEUDT sensor was evaluated by sensing humidity.

In a SAW sensor, three mechanisms contribute to sensor response, namely, mass loading and the viscoelastic and the acoustoelectric effects.⁸ The phase velocity shift and attenuation of a SAW that incorporate a thin film on the surface are obtained from perturbation theory.⁹ The expression for the phase velocity yields the influence of all three mechanisms, thus it is dependent on the mass, elasticity, and conductivity of the film. If one ignores changes in conductivity, the absorption of material will result in a decrease in frequency due to mass loading and to an increase in frequency due to larger elastic film values. The changes in phase velocity v can be measured as a change in frequency f of an oscillating circuit by employing a SAW delay line.

Even though SAWs are sensitive to any change in mechanical or electrical boundary conditions, it is the mass loading effect that is most often used in chemical sensor devices, i.e., disregarding possible changes in the elastic constants of the film and changes in conductivity. Then, the appropriate measure of sensor performance is the fractional frequency shift $\Delta f/f_0$ caused by a change in the mass deposited on the surface, given by

$$\Delta f/f_0 = -(k_1 + k_2) \cdot f_0 \cdot h \cdot \Delta \rho,$$

where $\Delta \rho$ is the change in mass density.¹⁰ k_i are frequency-independent constants that are proportional to the square of particle displacement (out of plane and in plane in the propagation direction, respectively). It should be noted that acoustic modes that have other oscillation polarizations will react differently on a particular load and thus give rise to some specificity of the chemical species. Due to $\Delta f \sim f^2$, and assuming a linear increase of the noise level with the frequency, higher frequencies improve the signal-to-noise ratio of the shift in frequency Δf proportional to f . The sensitivity enhancement has been demonstrated by comparison of 80 MHz and 1 GHz measurements using a sensitive coating (cyclodextrin) such that aromatic hydrocarbons can be easily

^{a)}Electronic mail: hesjedal@pdi-berlin.de

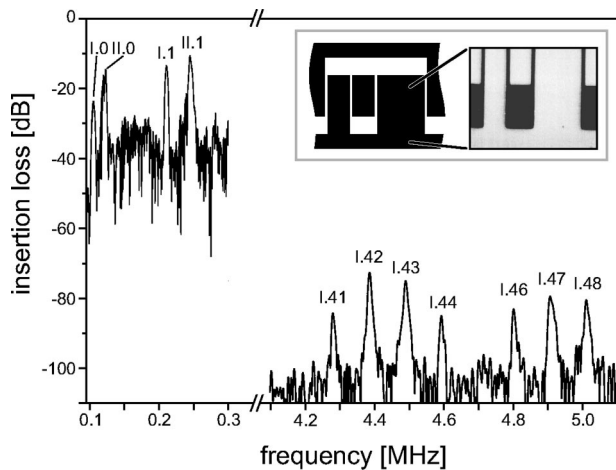


FIG. 1. SAW sensor device: A NG-FEUDT transducer is employed for efficient excitation of higher harmonics of two acoustic modes, as shown in the electrical transmission spectrum. The superscript (I/II) denotes the type of mode and the subscript ($n=1, \dots$) the order of harmonic excitation. The geometry of the NG-FEUDT structure (sketch and optical micrograph shown in the inset) is repeated 20 times ($\lambda=35 \mu\text{m}$). The device was fabricated by standard photolithography.

detected down to 1 ppm.⁵ The above expression is very similar to the equation for the shift in frequency derived for quartz resonators. As early as the 1950s Sauerbrey demonstrated the capability of a quartz crystal microbalance to determine small added mass loads.¹¹ The disadvantage of this successful thin film thickness measurement technique is the frequency limitation of 5–50 MHz compared to the 0.050–10 GHz that is in principle possible for SAW sensors.

Although high frequencies (small wavelengths), particularly those above 1 GHz, are essential for increasing sensitivity application of them is rarely reported.^{5,12} One reason is the difficulty to fabricate GHz SAW devices. For example, in order to achieve operating frequency of 5 GHz with single finger interdigital transducers (IDTs) with two electrodes per wavelength, with equal widths for the electrodes and gaps and a phase velocity of 3000 m/s, structural dimensions of roughly $0.15 \mu\text{m}$ have to be fabricated. Alternatively, higher phase velocity materials, like sputtered AlN films,¹³ can be employed that increase the frequency achievable using the same structural dimensions. Because standard optical photolithography is limited to about $0.5 \mu\text{m}$, the IDTs are usually operated at higher harmonics of fundamental frequency.¹² However, the efficiency of SAW excitation at higher harmonics in conventional device structures rapidly decreases so that their operation rarely reaches several GHz.

The effectiveness of the excitation of higher harmonics depends on the metallization ratio, i.e., smaller gap widths allow more efficient excitation of SAWs.¹⁴ Additionally, the use of unidirectional transducers reduces the insertion loss by 3 dB. Narrow gap-floating electrode unidirectional SAW transducers (NG-FEUDTs) were developed in 1984 by Yamanouchi and Furuyashiki.¹⁵ Their main advantages are higher operation frequencies for the same electrode width compared to conventional IDTs with a metallization (line-to-space) ratio of 1:1, smaller electrode resistance due to wider electrodes, and efficient excitation of higher harmonics due to the larger metallization ratio.

In Fig. 1, the geometry of a five-electrode NG-FEUDT

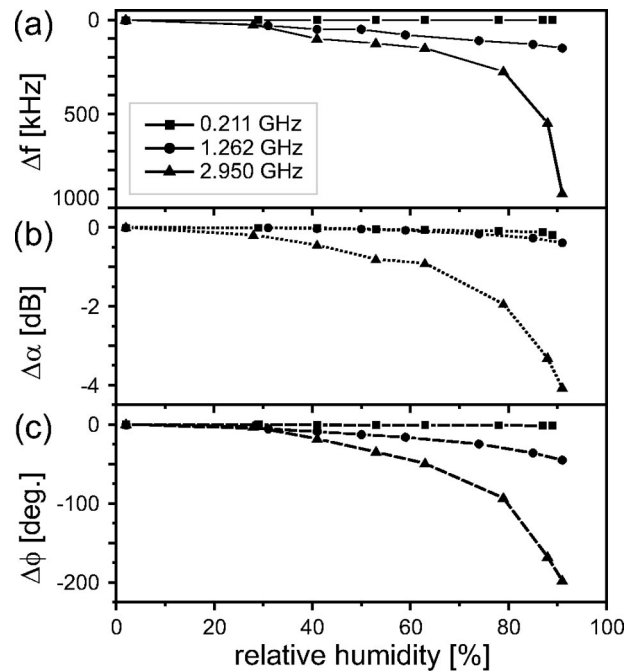


FIG. 2. Humidity dependence of selected peaks at $f=0.211$ (I.2), 1.262 (I.12), and 2.950 GHz (I.28). Frequency shift Δf , attenuation $\Delta\alpha$, and phase shift $\Delta\phi$ as a function of the RH.

structure is shown. The sensor structure was fabricated by conventional photolithography on *Y*-cut LiNbO₃ and propagation in the *X* direction (Euler angles: $0^\circ, 90^\circ, 0^\circ$). The metal electrodes (Ti–Al–Ti) have a total thickness of 60 nm. In the *X* direction, two acoustic modes are found, depending on the polarization of the oscillation. The first mode (I) is a Rayleigh-type wave with a calculated phase velocity of 3717.851 m/s and an electromechanical coupling coefficient of 1.4%. The oscillation components in the propagation direction (u_1), in plane and perpendicular to the direction of propagation (u_2), and in the out-of-plane direction (u_3) have a ratio of 3.2:1:4.5 on the electrically open surface, i.e., a Rayleigh-type mode with a small shear wave component. The second mode (II) at 4645.201 m/s (an electrically open substrate) shows different polarization: $u_1:u_2:u_3 = 1.8:4.9:1$, i.e., a wave with a dominant shear wave character. The finger width was $6.3 \mu\text{m}$ and the gap $0.7 \mu\text{m}$, resulting in an acoustic wavelength of $35 \mu\text{m}$ at fundamental frequency f_0^{I} of 0.105 GHz and f_0^{II} of 0.121 GHz, respectively. The center-to-center spacing of the IDTs is 2.7 mm. The transmission spectrum (S_{12}) was obtained using a network analyzer (Hewlett Packard 8720D) and it confirms SAW excitation up to $f^{\text{I/II}} = n^{\text{I/II}} f_0^{\text{I/II}}$ with $n^{\text{I}}=48$ at frequency of 5 GHz, and $n^{\text{II}}=13$ at frequency of 1.4 GHz, respectively. The increase of insertion loss with n is mainly due to the electrical mismatch to 50Ω that increases with the frequency. Thus, FEUDT devices offer the possibility of GHz operation that employs conventional photolithography. Moreover, the use of soft lithography techniques, like nanoimprint lithography¹⁶ or near-field phase shift lithography, opens the way for simple low-cost SAW devices operating up to 10 GHz.⁷

To test basic operation of the FEUDT sensor, a simple test system was set up. Water-vapor free pure N₂ was blown at a constant rate (1 sccm, controlled by a mass-flow control-

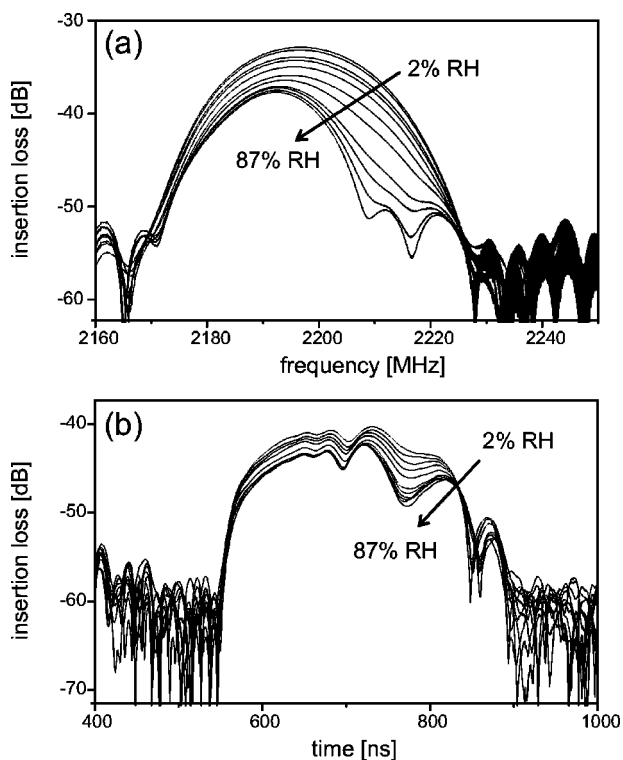


FIG. 3. Humidity dependence of the transmission curve at 2.203 GHz (f_{21}^1) in the (a) frequency and (b) time domains.

ler) into the test setup at a temperature of 24.6 °C. The test setup consists of the SAW sensor mounted on a high-frequency carrier chip, a temperature sensor and a capacitive hygrometer for comparison. To increase the relative humidity (RH) of the gas, part of the incoming gas is blown through a container of water and mixed with pure N₂. Figure 2 shows the shift in frequency Δf , attenuation $\Delta\alpha$, and phase shift $\Delta\Phi$ as a function of the RH in % for three selected frequencies. The first frequency analyzed $f(1)=0.211$ GHz corresponds to the second harmonic of the Rayleigh-type mode f_2^1 , $f(2)=1.262$ GHz corresponds to f_{12}^1 , and $f(3)=2.950$ GHz corresponds to f_{28}^1 . Frequency, attenuation, and phase react differently to changes of humidity, but reveal the same trends. The frequency shifts < 1, 150, and 923 kHz upon changing the humidity from 2% to 92% for $f(1)$, $f(2)$, and $f(3)$, respectively. The change in relative frequency $\Delta f/f$ at RH=92% (compared to at 2%) is thus roughly a linear function of f [$\Delta f(2)/f(2)=0.119\times 10^{-3}$ and $\Delta f(3)/f(3)=0.313\times 10^{-3}$]. The attenuation change $\Delta\alpha$ of the wave, which is caused by the film's conductivity, is 0.19, 0.39, and 4.08 dB for RH of 92% (compared to 2% RH). The change in phase at resonance frequency is evident for all frequency ranges with $\Delta f(1)=1.49^\circ$, $\Delta f(2)=45.17^\circ$, and especially for the highest frequency $\Delta f(3)=197.85^\circ$.

Taking a closer look at a single transmission peak reveals in more detail the response to water layer absorption. Figure 3 shows the humidity dependence of the transmission

at $f=2.203$ GHz in the frequency and time domains. At low humidity, the transmission in the frequency domain shows a broad peak that shifts towards lower frequencies with an increase in water absorption. At higher humidities, the peak splits into several weaker maxima. In the time domain, the effect of absorption is even more pronounced in the peak structure. A broad transmission signal is present at all humidities from 550 to 880 ns. Several distinct peaks can be identified ($t=650, 680, 720, 800,$ and 860 ns) that react differently on humidity: the faster peaks shift towards shorter times, and the slower peaks (800 and 860 ns) towards larger values of time. The analysis of the transmission spectrum in the time domain may thus offer another approach to the study of absorption.

Of course, the humidity sensing properties of this simple system can be largely improved by employing coatings. One example is coating with a layer of polyvinyl alcohol, followed by a layer of polystyrene sulfonic acid sodium, which was reported to increase the sensitivity to humidity by 180%.¹⁷

In this letter, we have demonstrated a simple easy-to-fabricate multimode multifrequency SAW sensor for the GHz frequency range. The sensor was tested as a hygrometer. In the future, this system will be applied to chemical sensing with suitable application of coatings, and may be able to replace conventional sensor arrays. Frequencies of up to 10 GHz will be explored for sensors, which may lead to even higher sensitivities. For this, we will employ "soft" lithography techniques for device fabrication. Also, different combinations of modes in layered systems will be screened for optimal liquid sensing properties.

The authors acknowledge the help of H. Kostial and Y. Takagaki for critical reading of the manuscript.

¹H. Wohltjen and R. Dessy, *Anal. Chem.* **51**, 1465 (1979).

²A. Bryant, D. L. Lee, and J. F. Vetelino, *1981 Ultrasonics Symposium Proceedings* (IEEE, New York, 1981), p. 171.

³D. S. Ballantine, R. M. White, S. I. Martin, A. J. Ricco, E. T. Zellers, G. C. Frye, and H. Wohltjen, *Acoustic Wave Sensors: Theory, Design, and Physico-Chemical Applications* (Academic, San Diego, 1997).

⁴B. Jakoby, *2000 Ultrasonics Symposium Proceedings* (IEEE, New York, 2000), p. 207.

⁵F. L. Dickert, P. Forth, W.-E. Bulst, G. Fischerauer, and U. Knauer, *Sens. Actuators B* **46**, 120 (1998).

⁶A. J. Ricco and S. J. Martin, *Sens. Actuators B* **10**, 123 (1993).

⁷T. Hesjedal and W. Seidel, *Nanotechnology* **14**, 91 (2003).

⁸A. J. Ricco and S. J. Martin, *Thin Solid Films* **206**, 94 (1991).

⁹B. A. Auld, *Acoustic Fields and Waves in Solids* (Wiley, New York, 1973).

¹⁰H. Wohltjen, *Sens. Actuators* **5**, 307 (1984).

¹¹G. Sauerbrey, *Z. Phys.* **155**, 206 (1959).

¹²A. C. Stevenson, H. M. Mehta, R. S. Sethi, L.-E. Cheran, M. Thompson, I. Davies, and C. R. Lowe, *Analyst* (Cambridge, U.K.) **126**, 1619 (2001).

¹³C. Caliendo and P. Imperatori, *Appl. Phys. Lett.* **83**, 1641 (2003).

¹⁴H. Engan, *IEEE Trans. Electron Devices* **ED-16**, 1014 (1969).

¹⁵K. Yamanouchi and H. Furuyashiki, *Electron. Lett.* **20**, 989 (1984).

¹⁶Y. Takagaki, E. Wiebicke, H. Kostial, and K. H. Ploog, *Nanotechnology* **13**, 15 (2002).

¹⁷S. Furukawa, M. Obana, and T. Nomura, *1995 IEEE Ultrasonics Symposium Proceedings* (IEEE, New York, 1995), p. 539.